Virtual Screening Studies to Design Potent CDK2-Cyclin A Inhibitors

S. Vadivelan,*[,†,‡] Barij Nayan Sinha,[‡,#] Sheeba Jem Irudayam,[§] and Sarma A. R. P. Jagarlapudi[†]

GVK Biosciences Pvt. Ltd. S-1, Phase-1, T.I.E. Balanagar, Hyderabad-500037, India, Department of Pharmaceutical Sciences, Birla Institute of Technology, Mesra-835215, Ranchi, India, Manchester Interdisciplinary Biocentre, The University of Manchester, 131 Princess Street, Manchester M1 7DN, United Kingdom, and School of Chemistry, The University of Manchester, Oxford Road, Manchester M13 9PL, United Kingdom

Received February 23, 2007

The cell division cycle is controlled by cyclin-dependent kinases (CDK), which consist of a catalytic subunit (CDK1−CDK8) and a regulatory subunit (cyclin A−H). Pharmacophore analysis indicates that the best inhibitor model consists of (1) two hydrogen bond acceptors, (2) one hydrogen bond donor, and (3) one hydrophobic feature. The HypoRefine pharmacophore model gave an enrichment factor of 1.31 and goodness of fit score of 0.76. Docking studies were carried out to explore the structural requirements for the CDK2−cyclin A inhibitors and to construct highly predictive models for the design of new inhibitors. Docking studies demonstrate the important role of hydrogen bond and hydrophobic interactions in determining the inhibitor-receptor binding affinity. The validated pharmacophore model is further used for retrieving the most active hits/lead from a virtual library of molecules. Subsequently, docking studies were performed on the hits, and novel series of potent leads were suggested based on the interaction energy between CDK2−cyclin A and the putative inhibitors.

INTRODUCTION

Uncontrolled cell proliferation, a hallmark of cancer, may result from an increased expression of cell cycle up-regulators from a reduced expression of cell cycle down-regulators, or both. The effects of CDK inhibitors on the cell cycle and their potential value for the treatment of cancer have been extensively studied.[1−3] The properties that make CDK inhibitors attractive as potential antitumor agents are (1) they are potent antiproliferative agents, arresting cells in G1 or G2/M phase, (2) they trigger apoptosis, alone or in combination with other treatments, and (3) in some instances, inhibitors of CDKs contribute to cell differentiation. The importance of these kinase pathways is highlighted by the fact that the genes encoding CDK, their cyclin partners, or their endogenous peptide inhibitors are mutated in a large proportion of human tumors. Many reports have been published describing various CDK inhibitors and their interactions that are important for the treatment of cancer.[4−7] Consequently, many inhibitors are being synthesized, but most of them are only in the "discovery" phase. The known CDK inhibitors[4] fall into three classes: (1) those that are not selective for any specific CDK (for example, deschloroflavopiridol, flavopiridol, oxindole 16, and oxindole 91), (2) those that inhibit CDK1, 2, 5 (for example, olomoucine, (*R*)-roscovitine, purvalanol B, aminopurvalanol (NG97), hymenialdisine, indirubin-3′-monoxime, indirubin-5-sulfonate, SU9516, and alsterpaullone), and (3) those that are selective for CDK4, 6 (for example, fascaplysin, PD0183812, and CINK4). Some of the potent CDK inhibitors are shown in Scheme 1. No selective inhibitor of CDK has been discovered yet, possibly because of the conservation of the amino acids lining the CDK ATP-binding pocket. Despite striking chemical diversity, all CDK inhibitors share some common properties: they have low molecular weights (<600), they are flat, hydrophobic heterocycles, they act by competing with ATP for binding in the ATP-binding site, and they bind by hydrophobic interactions and hydrogen bonds with the kinase. The interactions that favor the inhibition of the protein by a ligand are hinge interactions, polar interactions, and hydrophobic interactions. The importance of the hydrogen bond interactions with the hinge segment of the kinase for inhibitor binding is consistent with the presence of crystallographically determined water molecules forming a hydrogen bond network with the backbone of Glu 81 and Leu 83 in the structure of the apoenzyme. The work done shows how chemical features for a set of CDK2−cyclin A inhibitors, along with their activities, which range over several orders of magnitude, can be used to generate pharmacophore hypotheses and can successfully predict the activity. The validated pharmacophore model is used to retrieve molecules from a virtual library, and the retrieved hits/leads were further refined using docking studies to reduce the number of false positives and false negatives. This virtual screening approach can be used to identify and design inhibitors with greater selectivity.

COMPUTATIONAL DETAILS

A. Pharmacophore Studies using Catalyst. Three hundred twenty-six human CDK2−cyclin A inhibitors from literature[8−44] were selected for the pharmacophore develop-

* To whom correspondence should be addressed. Phone: (91) 9849727728. Fax: (91) 4023721010. E-mail: vadivelan@gvkbio.com.
† GVK Biosciences Pvt. Ltd.
‡ Birla Institute of Technology.
§ The University of Manchester.
# Current address: Department of Pharmaceutical Sciences, Birla Institute of Technology, Mesra-835215, Ranchi, India.

10.1021/ci7000742 CCC: $37.00
Published on Web 05/25/2007

Scheme 1. Some of the Potent CDK Inhibitors[4]

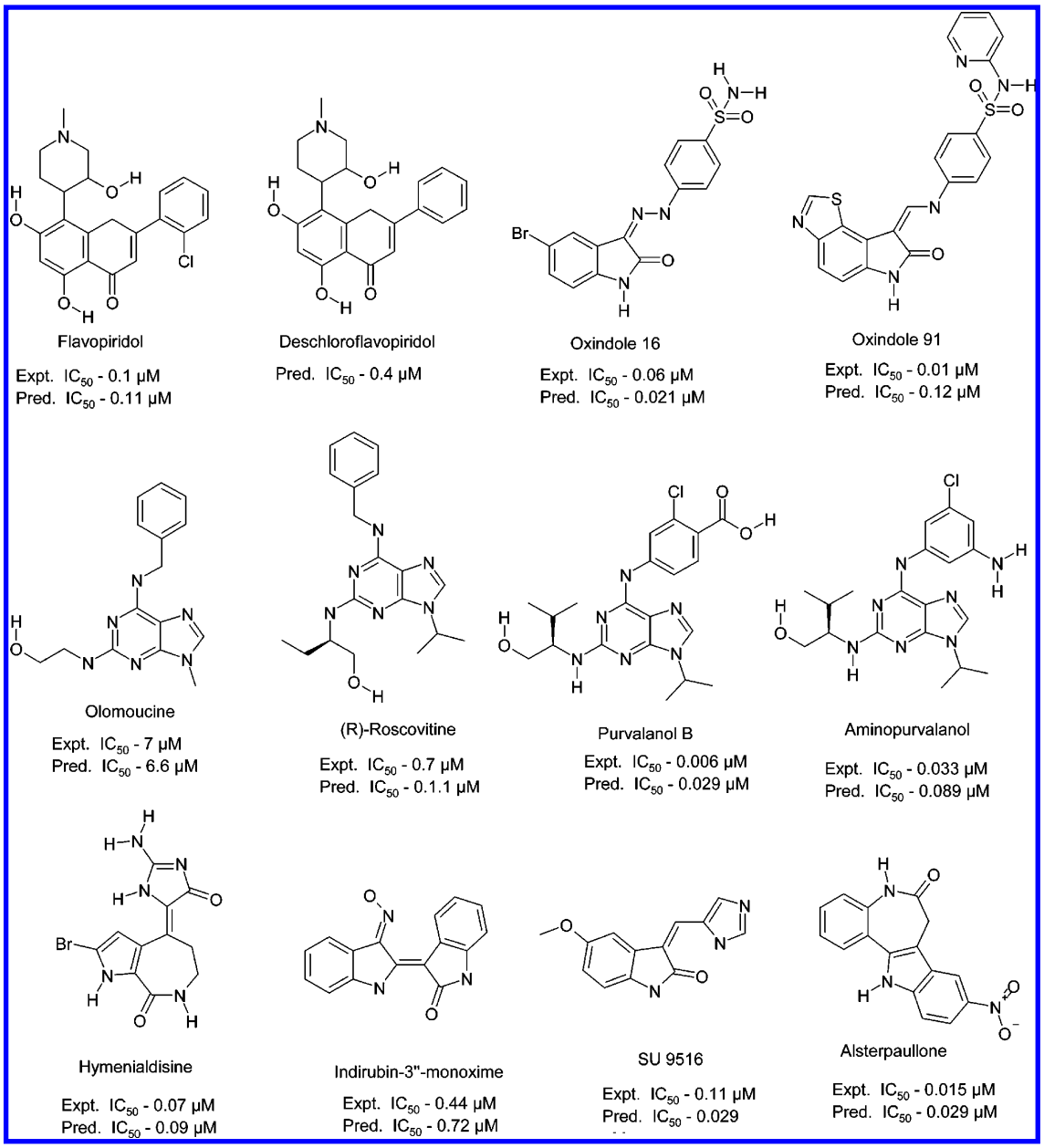

ment studies using Catalyst.[45] Although the biological data was obtained from different publications, the assay method used in all the publications is same. The IC_{50} values for a standard molecule, such as olomoucine, against the CDK2−cyclin A complex are reported to have the same value (7 μM) in about 11 publications used in this study. Also, few other standard molecules were reported with same biological activity in the remaining publications. This indicates that the data reported across the reference articles is same and needs no normalization. Twenty-four molecules were selected in the training set based on diversity without any redundancy in information content in terms of both structural features and activity ranges. The molecules selected as the training set are given in Figure 1, and a few molecules from the test set are given in Figure 2. HipHop identifies the common chemical features necessary for a molecule to be biologically active. Therefore, a qualitative model from HipHop was generated with six most-active molecules with diverse scaffolds from the training set (**1**, **2**, **3**, **4**, **5**, and **6**). However, these models cannot be directly used for quantitative estimation of activities for the molecules screened from other databases or sets. A training set of 24 molecules was used to generate HypoGen pharmacophore models, which could be used for quantitative estimation of activities, while screening large virtual compound libraries. While generating the HypoGen model, a minimum number of features involving hydrogen bond acceptor, hydrogen bond donor, and hydrophobic moieties were specified on the basis of common feature identification. The molecules in the training set were broadly classified into three categories, namely, highly active (<1 μM), moderately active (1−10 μM), and inactive (>10 μM). The quality of the HypoGen models are best described by Debnath[46] in terms of fixed cost, null cost, and total cost and other statistical parameters. According to which, a large difference between the fixed cost and null cost, and a value of 40−60 bits for the unit of cost would imply a 75−90% probability for experimental and predicted activity correlation. For any hypothesis to be a good model, the total cost

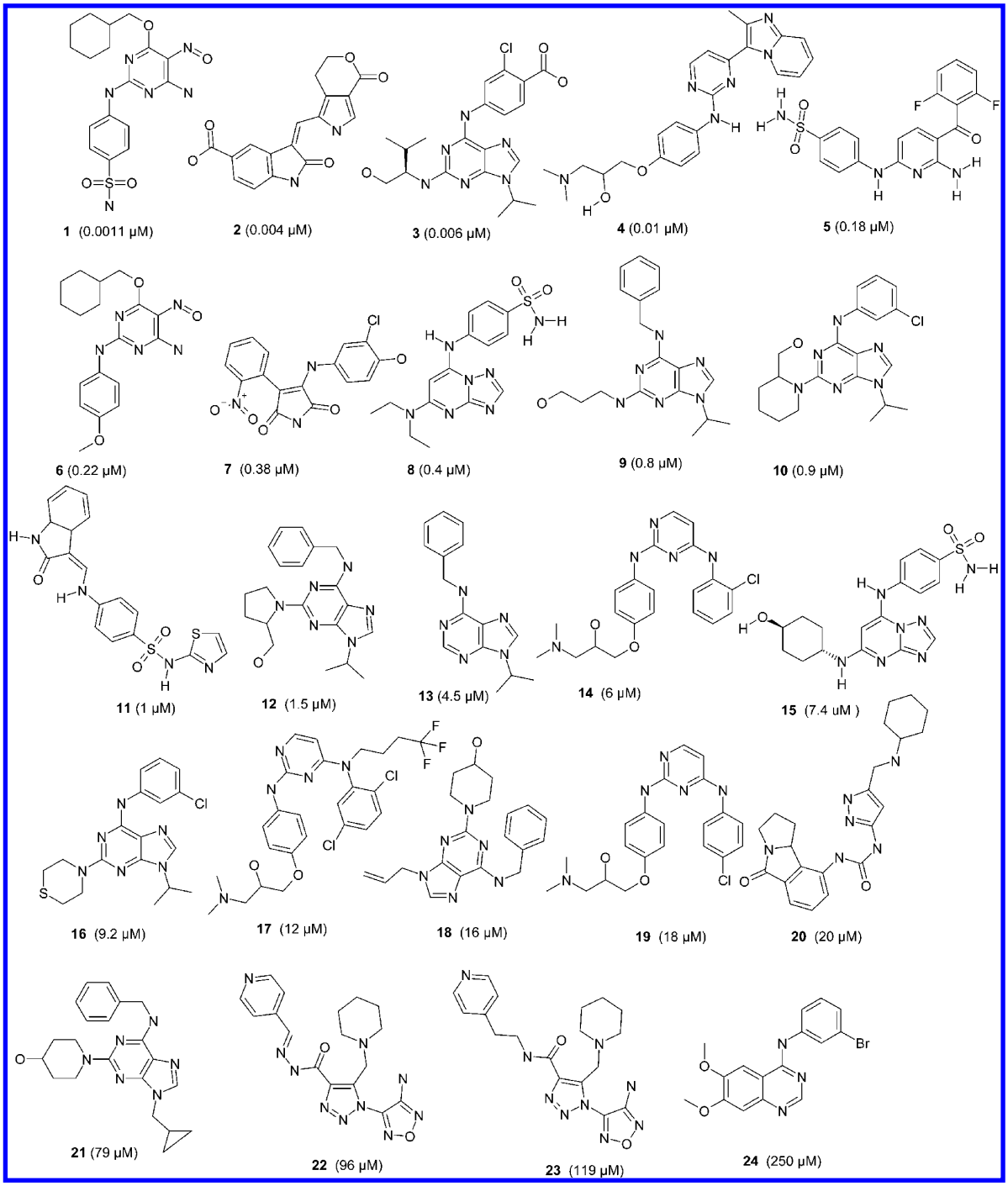

Figure 1. Training set molecules for CDK2−cyclin A inhibitors. IC_{50} values of each molecule are given in parentheses.

should be close to the fixed cost. The activity of the molecules used in the study depends to a greater extent on the steric nature of the substituents; hence, HypoRefine was performed with 1 as the value for excluded volume. In general, HypoRefine performs a simulated annealing refinement of pharmacophore models by generating excluded volumes. The generated model from HypoRefine was comparatively better than the HypoGen model and was used for further analysis.

B. Docking Studies Using GOLD. The crystal structure of CDK2−cylin A (PDB 2C5O) was used for the study. The protein 3D structure was downloaded from the protein databank (PDB);[47] the solvent molecules in the protein were removed. Hydrogen atoms were added to the protein using Cerius[2] module.[48] Structure-based docking studies were carried out using GOLD,[49] version 3.0, on CDK2−cyclin A inhibitors and on hits/leads from virtual screening to the 3D structure of CDK2−cyclin A complex. The active site was defined as the region within 12 Å from the geometric centroid of ligand ($x = 4.1$, $y = 48.4$, and $z = 2.06$) complexed with the protein CDK2−cyclin A. Docking was terminated when the conformational similarity had a rms deviation of less than 1.5 Å. The annealing parameter of van der Waal interactions was 4.0, and the cutoff distance to identify hydrogen interactions was 3.0 Å. Highly active hits retrieved from the virtual screening libraries were further refined by performing docking studies with the molecules.

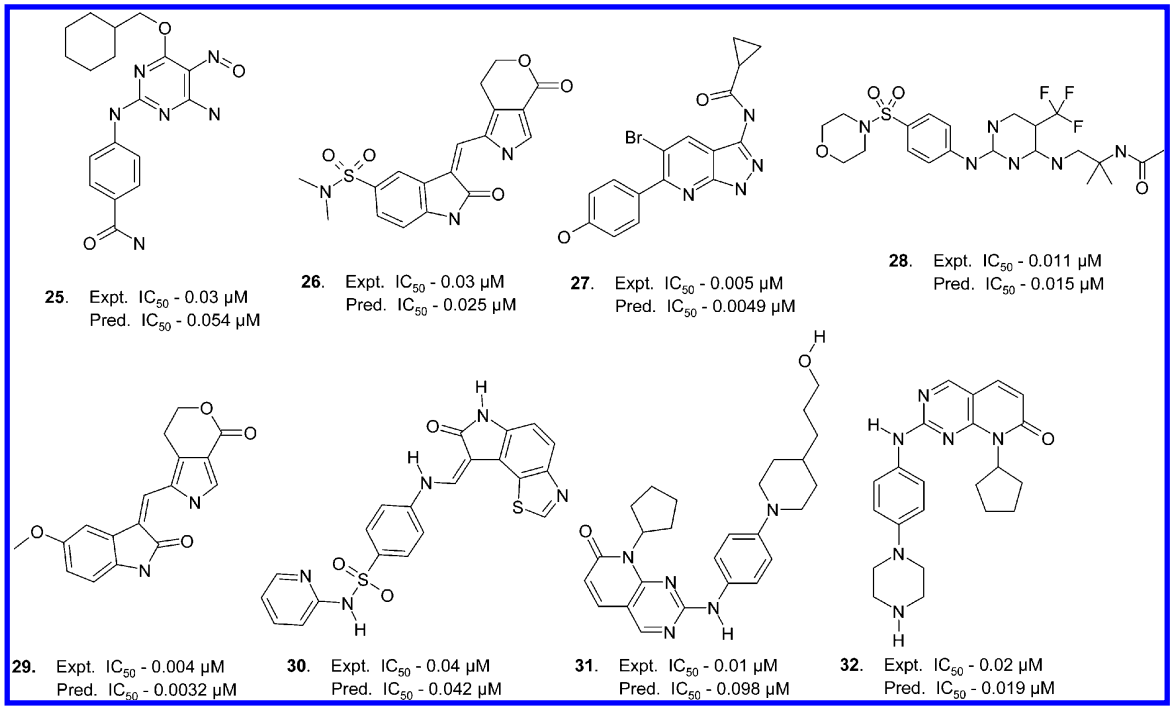

Figure 2. Some test set molecules for CDK2−cyclin A inhibitors along with its experimental and pharmacophore predicted IC_{50} values.

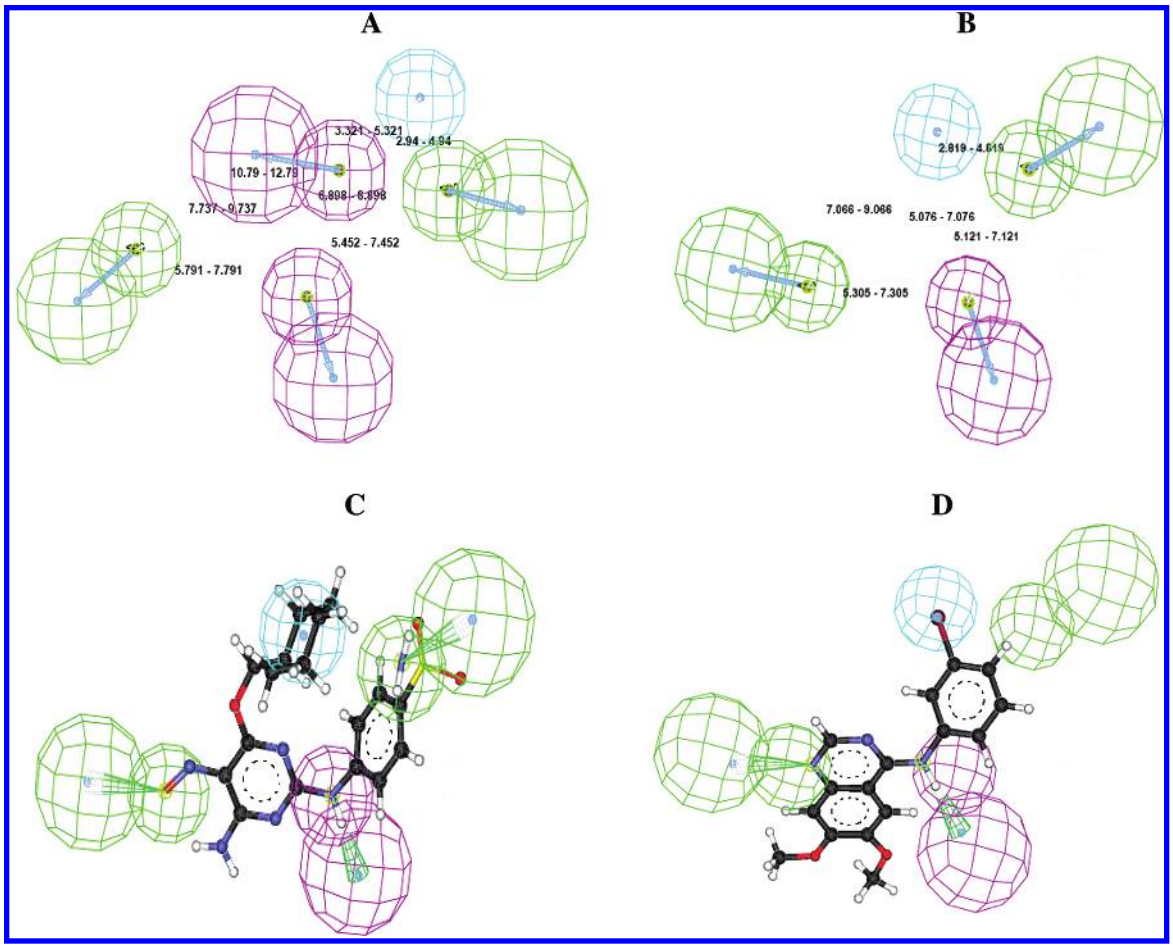

Figure 3. Pharmacophore model for CDK2−cyclin A inhibitors. (a) HipHop model displayed with the distance between the features. (b) HypoRefine features with its distance constraints. (c) Pharmacophore mapped to the most active molecule (**1**, 0.0011 μM). (d) Pharmacophore mapped to the least active molecule (**24**, 250 μM). Features are color coded with green, one hydrogen bond acceptor; magenta, hydrogen bond donor; and light blue, one hydrophobic feature.

Table 1. Ten Pharmacophore Models Generated by the HypoRefine for CDK2−Cyclin A Inhibitors

hypo no.	total cost	cost difference[a]	error cost	rms deviation	training set (*r*)	features[b]
1	80.15	59.55	61.88	0.827	0.949	AADH
2	89.02	50.68	71.44	1.099	0.941	AADH
3	90.29	49.41	71.96	1.113	0.938	AADH
4	90.56	49.14	71.27	1.295	0.953	AADH
5	91.47	48.23	75.07	1.310	0.942	AADH
6	92.83	46.87	74.70	1.402	0.946	AAAH
7	92.49	47.21	75.61	1.445	0.934	AAAH
8	92.24	47.46	75.93	1.475	0.921	AADH
9	92.48	47.22	76.91	1.418	0.914	AADH
10	92.51	47.19	76.78	1.416	0.905	AADH

[a] (Null cost − total cost), null cost = 139.70, fixed cost = 95.75, For Hypo-1, weight = 1.67, configuration = 13.90. All cost units are in bits. [b] A = hydrogen bond acceptor, D = hydrogen bond donor, H = hydrophobic feature.

Table 2. Experimental and Predicted IC_{50} Data of 24 Training-Set Molecules against the HypoRefine Model

molecule	exptl IC_{50} (μM)	predicted IC_{50} (μM)	error[a]	fit value[b]	exptl scale[c]	predicted scale[c]
1	0.0011	0.0057	5.2	10.17	+++	+++
2	0.004	0.029	7.2	9.46	+++	+++
3	0.006	0.029	4.9	9.46	+++	+++
4	0.01	0.062	6.2	9.13	+++	+++
5	0.18	0.046	−3.9	9.26	+++	+++
6	0.22	0.13	−1.7	8.8	+++	+++
7	0.38	0.73	1.9	8.07	+++	+++
8	0.4	0.15	−2.7	8.76	+++	+++
9	0.8	3	3.8	7.45	+++	++
10	0.9	0.73	−1.2	8.06	+++	+++
11	1	1.8	1.8	7.66	++	++
12	1.5	1	−1.4	7.91	++	++
13	4.5	32	7.1	5.42	++	+
14	6	2.4	−2.5	7.55	++	++
15	7.4	3.2	−2.3	7.42	++	++
16	9.2	7.3	−1.3	7.06	++	++
17	12	5.7	−2.1	7.17	+	++
18	16	4.4	−3.7	7.29	+	++
19	18	7.3	−2.4	7.06	+	++
20	20	2.5	−8	7.53	+	++
21	79	110	1.3	5.9	+	+
22	96	51	−1.9	6.22	+	+
23	120	41	−2.9	6.32	+	+
24	250	34	−7.4	6.4	+	+

[a] A positive value indicates that the predicted IC_{50} is higher than the experimental IC_{50}, while a negative value indicates that the predicted IC_{50} is lower than the experimental IC_{50}; a value of 1 indicates that the predicted IC_{50} is equal to the experimental IC_{50}. [b] Fit value indicates how well the features in the pharmacophore overlap the chemical features in the molecule. Fit = weight × [max(0,1 − SSE)], where SSE = $(D/T)2$, D = displacement of the feature from the center of the location constraint and T = the radius of the location constraint sphere for the feature (tolerance). [c] Activity scale: $IC_{50} < 1$ μM, +++ (highly active); $IC_{50} = 1-10$ μM, ++ (moderately active); $IC_{50} > 10$ μM, + (low active).

RESULTS AND DISCUSSION

Pharmacophore Studies. The best HipHop[50] pharmacophore model indicated the importance of hydrogen bond acceptors, hydrogen bond donors, and hydrophobic features which were further confirmed in the HypoRefine generated models. This study resulted in 10 hypothesis models with good cost values, correlation (*r*) and root-mean-square deviations (RMSD) between the experimental and predicted activities, which are given in Table 1. The hypothesis with highest cost difference (59.55 bits), the lowest RMSD value

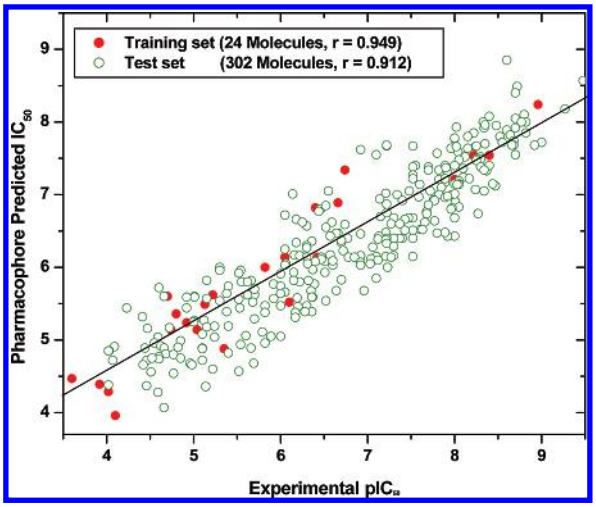

Figure 4. Graph showing the correlation (*r*) between experimental and predicted activities for the 302 test set molecules against the Hypo-1 model along with 24 training set molecules for CDK2−cyclin A inhibitors.

Table 3. Statistical Parameters from Screening of Test Set Molecules

	parameter	CDK2−cyclin A
1	total molecules in database (D)	302
2	total no. of actives in database (A)	213
3	total hits (Ht)	217
4	active hits (Ha)	201
5	% yield of actives [(Ha/Ht) × 100]	92.63
6	% ratio of actives [(Ha/A) × 100]	94.37
7	enrichment factor (E) [(Ha × D)/(Ht × A)]	1.31
8	false negatives [A − Ha]	12
9	false positives [Ht − Ha]	16
10	goodness of hit score[a]	0.76

[a] [(Ha/4HtA)(3A+Ht)) ×(1 − ((Ht − Ha)/(D − A))]; GH Score of 0.7−0.8 indicates a very good model.

(0.827), and correlation of 0.949 was characterized as the best hypothesis. The fixed cost, pharmacophore (total) cost, and null cost for this hypothesis are 95.75, 80.15, and 139.71 bits, respectively. It is evident that because error, weight, and configuration components are very low and not deterministic to the model, the total pharmacophore cost is also low and close to the fixed cost. Also, because the total cost is less than the null cost, this model accounts for all the pharmacophore features and has good predictive ability. Figure 3a and b shows the HipHop and HypoRefine pharmacophore features with their geometric parameters. Figure 3c and d represents the HypoRefine model aligned with the most active and inactive molecules (**1** and **24**) with IC_{50} values of 0.0011 and 250 μM, respectively. In molecule **1**, the two hydrogen bond acceptors were mapped to the nitroso and sulfonyl groups; the hydrogen bond donor was mapped to 2-aminopyrimidine group, and hydrophobic contour wasmapped to the cyclohexyl group. In molecule **24**, one of the hydrogen bond acceptors and the hydrophobic contours were not mapped, while one hydrogen bond acceptor mapped to 4-amino quinazoline and a hydrogen bond donor mapped to first position tertiary nitrogen of quinazoline. Analyzing the results, we observed that out of 10 highly active molecules, one was predicted to be moderately active, and the rest were predicted correctly as highly active. For the six moderately active molecules, except one, which was predicted as inactive, five were correctly

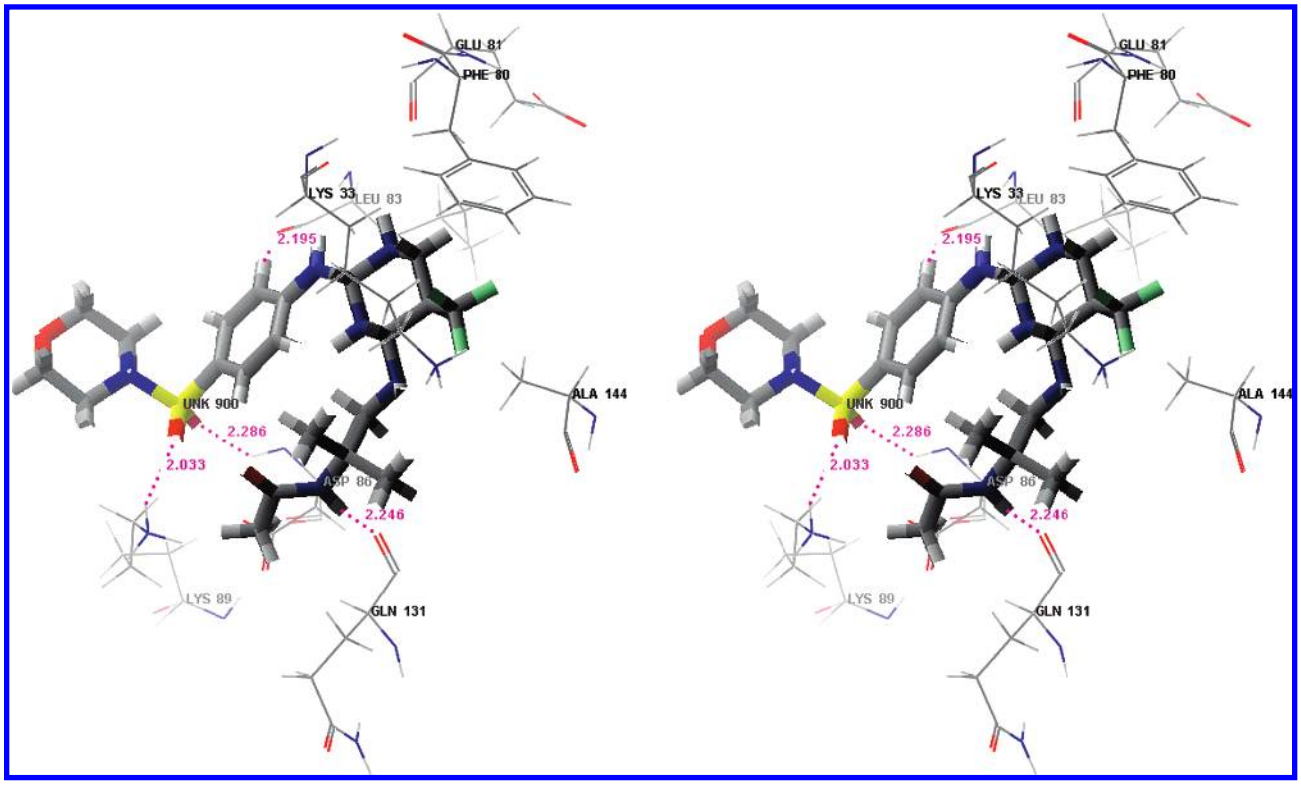

Figure 5. Stereoview of the binding mode of molecule **28** in the ATP-binding site of CDK2−cyclin A, suggested by molecular docking studies. Molecule **28** and its H-bonding patterns (LEU83, ASP86, LYS89, and GLN131) are represented with a stick and line model. The key H-bonds between **28** and CDK2−cyclin A are indicated by the pink dotted lines, together with the bond lengths in angstroms. The atoms are colored as follows: H, white; O, red; N, blue; C, gray.

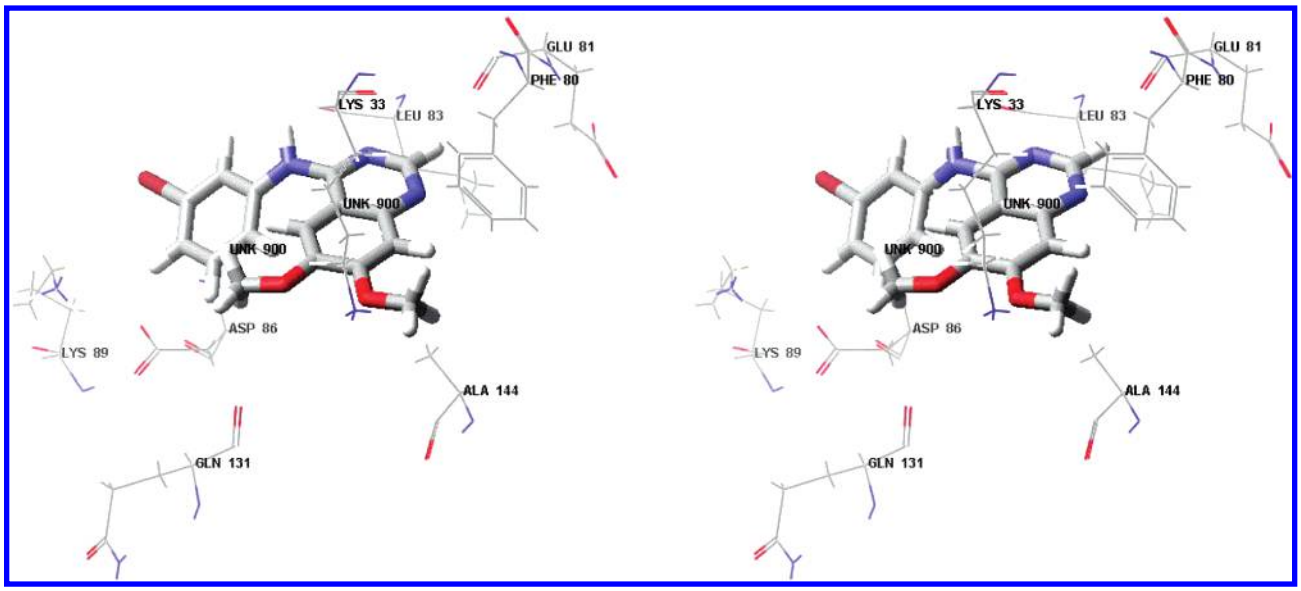

Figure 6. Stereoview of molecule **24** in the ATP-binding site of CDK2−cyclin A, suggested by molecular docking studies. The atoms are colored as follows: H, white; O, red; N, blue; C, gray.

predicted. Out of eight inactive molecules, only four were correctly predicted as inactive, and the rest were predicted as moderately active. The experimental and predicted activities along with the error and fit values for the training set molecules are given in Table 2. The correlation values along with the predictions above make the pharmacophore suitable to predict molecular properties well. The plot showing the correlation between the actual and predicted activity for the test set and the training set molecules is given in Figure 4. The activity of the test set molecules was also scored using the best hypothesis generated, and the results gave a correlation value of 0.912. This indicates that the pharmacophore model generated is capable of predicting the activity of the unknown molecules with reasonable accuracy.

Model Validation. The purpose of the pharmacophore model generation is not just to predict the activity of the training set compounds accurately but also to verify whether the pharmacophore models are capable of predicting the activities of external compounds of the test set series and classifying them correctly as active or inactive. The best pharmacophore hypothesis was used initially to screen the 302 CDK2 inhibitors. All queries were performed using the

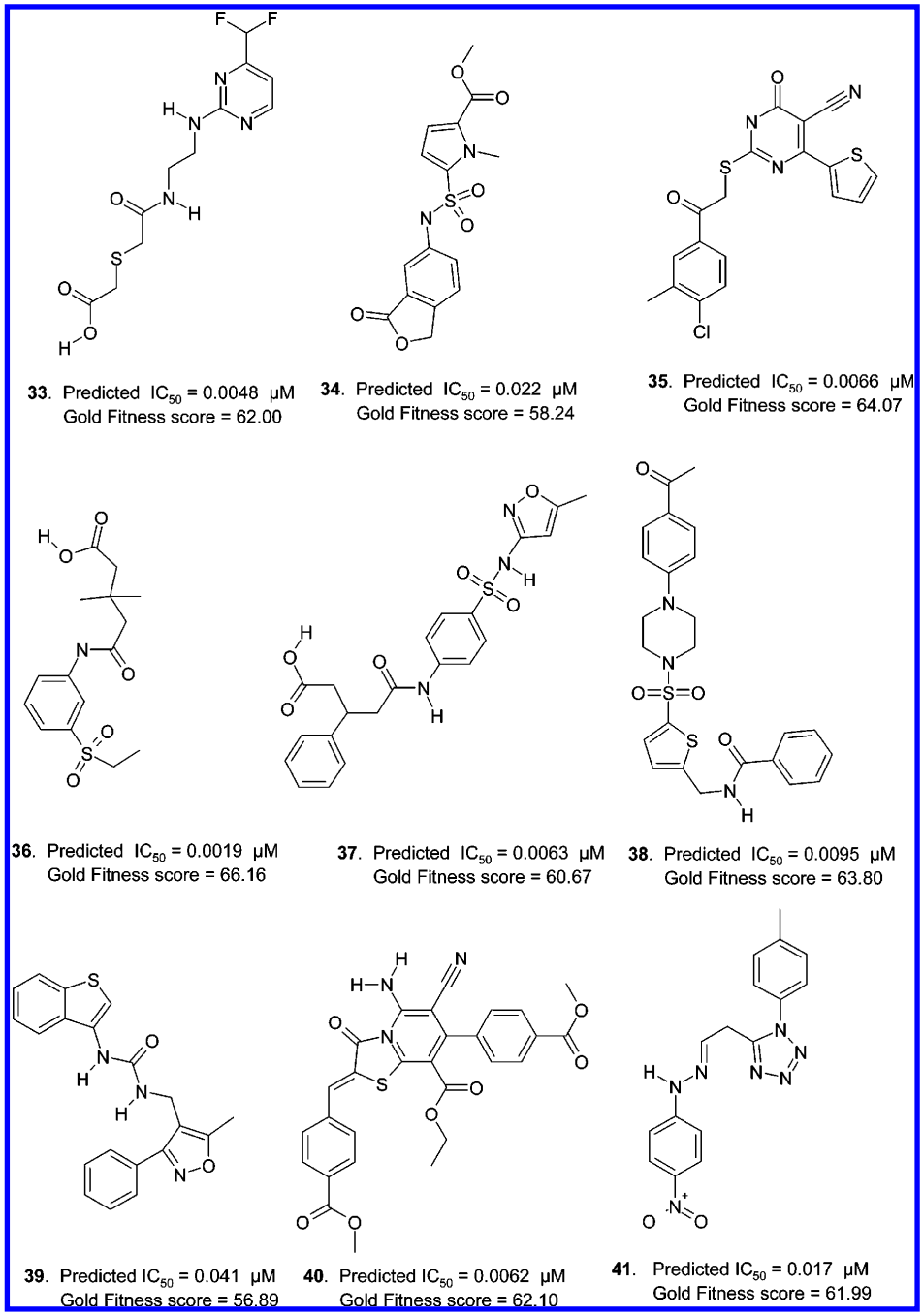

Figure 7. Lead molecules retrieved from the NCI database as potent CDK2−cyclin A inhibitors along with the pharmacophore predicted IC_{50} and GOLD fitness score values.

best flexible search databases/spreadsheet method. Hypo-Refine 1 was used to screen the known high-, medium-, and low-active inhibitors of the test set. Database mining was performed with catalyst software using the BEST flexible searching technique. A number of parameters,[51] such as hit list (Ht), number of active percent of yields (%Y), percent ratio of actives in the hit list (%A), enrichment factor of (E), false negatives, false positives, and goodness of hit score (GH) were calculated (Table 3) while the database mining of test set molecules was carried out. The number of molecules in the database is 302, and of these, 213 are highly active, 54 are moderately active, and 35 are low-active compounds. While the false positives and negatives, 16 and 12, respectively, are minimal, the enrichment factor of 1.31 is a very good indication of the high efficiency of the screening. Of the 213 highly active molecules, 15 were predicted as moderately active and four were predicted as least active. In the 54 moderately active molecules, six were predicted as low active and three as highly active; the rest (45) were correctly predicted. The model also predicted three of the low active molecules as moderately active and two more molecules from the same set as highly active. Thus, the features of HypoRefine 1 are relatively well optimized. However, in the case of highly active molecules, there are bulky groups present which may decrease the ability of the HypoRefine to select the most highly active molecules.

Docking Studies. Docking was performed on the 326 CDK2−cyclin A inhibitors and also on hits retrieved from virtual screening using GOLD. Fifty distinct poses of each ligand in the active site of CDK2−cyclin A were generated.

GOLD fitness scores were compared with observed activity for all molecules which were found to correlate well with the biological activities (326 molecules, $r = 0.591$). The most active molecules are found to have a very high fitness score. It was also observed that hydrogen bond interactions play a major role in deciding the fitness score of the molecule. A better understanding of the interactions is obtained by viewing the molecules in the active site. The most energetically favorable conformation for molecule **28** (Boehringer Ingelheim, Discovery phase) in the CDK2−cyclin A complex is shown in Figure 5. It forms four different hydrogen bonding interactions with the amino acids in the hinge region and other active site amino acids of the CDK2−cyclin A complex. The NH moiety of the tertiary butyl group formed a hydrogen bond with backbone carbonyl group of GLN131 with an interaction distance of 2.246 Å. The aromatic C−H group formed an H-bond with backbone carbonyl of LEU83 with an interaction distance of 2.195 Å. Similarly, the sulfonyl group is hydrogen bonded to side chain amino group of LYS89 and the backbone amino group of ASP86 with distances of 2.033 and 2.286 Å, respectively. Most of the inhibitors had bulky substituents interacting with the hydrophobic ribose pocket. The most energetically favorable conformation for molecule **24** ($IC_{50} = 250\ \mu M$) in the ATP binding site of CDK2−cyclin A complex is shown in Figure 6. As evident from the figure, there is a complete absence of H-bond interactions in the ATP binding site of CDK2−cyclin A complex, which clearly suggests that molecule **24** is inactive.

Virtual Library Screening. The Hypo-1 model was used to screen the NCI database consisting of 238 819 molecules, which yielded 4927 hits comprising 324 high, 1726 medium, and 2877 low-active molecules. The high-active molecules were those with a value of $<1\ \mu M$; moderately active molecules had values of $1-10\ \mu M$, and those of inactive molecules were $>10\ \mu M$. Only 104 hits are found to have activities below the $0.01\ \mu M$ cutoff. In fact, one can consider all the 324 hits that are predicted as highly active as good options for further evaluation, but some others in the medium-active range cannot be completely neglected. Some of the hits with good predicted activities were further subjected to docking studies to reduce the number of false positives and false negatives. On the basis of the earlier observations and the model developed in this study, it is observed that this virtual screening effort produced relatively more hits on which further experimental studies could be carried out. A few of the lead molecules with high predicted activity and fitness score are given in Figure 7.

CONCLUSION

The pharmacophore models were capable of predicting the activities over a wide variety of scaffolds and thus can be used as (1) a three-dimensional query in database searches to identify compounds with diverse structures that can function as potent inhibitors and (2) to evaluate how well any newly designed compound maps to the pharmacophore before undertaking any further study including synthesis. Both these applications may help in the identification or design of compounds for further biological evaluation and optimization. Pharmacophore studies indicate that the best inhibitor model consists of (1) two hydrogen bond acceptors, (2) one hydrogen bond donor, and (3) one hydrophobic feature. The most-active molecule in the training set fits very well with the top scoring pharmacophore hypothesis. Virtual screening produced some false positives and a few false negatives. It is believed that concurrent use or a docking study, which readily minimizes these errors, could be an added tool for the pharmacophore model based virtual screening to produce reliable true positives and negatives. GOLD docking studies show the important interactions which the potent inhibitors have with the active site residues. The pharmacophore model is further used to screen putative molecules from the NCI database. An astute blend of pharmacophore analysis, docking procedures, and database searching has resulted in the prediction of putative novel inhibitors of the CDK2−cyclin A complex.

ACKNOWLEDGMENT

Vadivelan would like to thank D. S. Brar, Chairman, and G. V. Sanjay Reddy, CEO, of GVK Biosciences Pvt. Ltd. for their continuous support and S. Rama Devi, Aparna Vema, G. Madhavi Sastry, and Sunita Tajne for their guidance and technical support.

Supporting Information Available: Table of predicted and experimental IC_{50} values to test-set molecules. This material is available free of charge via the Internet at http://pubs.acs.org.

REFERENCES AND NOTES

(1) Radzio-Andzelm, E.; Lew, J.; Taylor, S. Bound to activate: Conformational consequences of cyclin binding to CDK2. *Structure* **1995**, *3*, 1135−1141.
(2) Furet, P. X-ray crystallographic studies of CDK2, a basis for cyclin-dependent kinase inhibitor design in anticancer drug research. *Curr. Med. Chem. Anti-Cancer Agents* **2003**, *3*, 15−23.
(3) Johnson, D. G.; Walker, C. L. Cyclins and cell cycle checkpoints. *Annu. Rev. Pharmacol. Toxicol.* **1999**, *39*, 295−312.
(4) Knockaert, M.; Greengard, P.; Meijer, L. Pharmacological inhibitors of cyclin-dependent kinases. *Trends Pharmacol. Sci.* **2002**, *23*, 417−425.
(5) Russo, A. A.; Jeffrey, P. D.; Pavletich, N. P. Structural basis of cyclin-dependent kinase activation by phosphorylation. *Nat. Struct. Biol.* **1996**, *3*, 696−700.
(6) Philip, D.; Jeffrey Alicia, A.; Russo.; Kornelia Polyak.; Emma Gibbs.; Jerard Hurwitz.; Joan Massague.; Nikola, P.; Pavletich. Mechanim of CDK activation revealed by the structure of a cyclin-A−CDK2 complex. *Nature* **1995**, *376*, 313−320.
(7) Benson, C.; Kaye, S.; Workman, P.; Garrett, M.; Walton, M.; de Bono, J. Clinical anticancer drug development: targeting the cyclin-dependent kinases. *Br. J. Cancer.* **2005**, *92*, 7− 12.
(8) Bramson, H. N.; Corona, J.; Davis, S. T.; Dickerson, S. H.; Edelstein, M.; Frye, S. V.; Gampe, R. T. Jr.; Harris, P. A.; Hassell, A.; Holmes, W. D.; Hunter, R. N.; Lackey, K. E.; Lovejoy, B.; Luzzio, M. J.; Montana, V.; Rocque, W. J.; Rusnak, D.; Shewchuk, L.; Veal, J. M.; Walker, D. H.; Kuyper, L. F. Oxindole-based inhibitors of cyclin-dependent kinase 2 (CDK2): Design, synthesis, enzymatic activities, and X-ray crystallographic analysis. *J. Med. Chem.* **2001**, *44*, 4339−4358.
(9) Oh, C.-H.; Lee, S.-C.; Lee, K.-S.; Woo, E.-R.; Hong, C. Y.; Yang, B.-S.; Baek, D. J.; Cho, J-H. Synthesis and biological activities of C-2, N-9-substituted 6-benzylaminopurine derivatives as cyclin-dependent kinase inhibitor. *Arch. Pharm. Pharm. Med. Chem.* **1999**, *332*, 187−190.
(10) Oh, C.-H.; Kim, H.-K.; Lee, S.-C.; Oh, C.; Yang, B.-S.; Rhee, H. J.; Cho, J-H. Synthesis and biological properties of C-2, C-8, N-9-substituted 6-(3-chloroanilino)-purine derivatives as cyclin-dependent kinase inhibitors. Part II. *Arch. Pharm. Pharm. Med. Chem.* **2001**, *334*, 345−350.
(11) Sielecki, T. M.; Johnson, T. L.; Jie-Liu.; Muckelbauer, J. K.; Grafstrom, R. H.; Cox, S.; Boylan, J.; Burton, C. R.; Chen, H.; Smallwood, A.; Chang, C.; Boisclair, M.; Benfield, P. A.; Trainor, G. L.; Seitz, S. P. Quinazolines as cyclin dependent kinase inhibitors. *Bioorg. Med. Chem. Lett.* **2001**, *11*, 1157−1160.

(12) Song, Y.; Wang, J.; Teng, S. F.; Kesuma, D.; Deng, Y.; Duan, J.; Wang, J. H.; Qi, R. Z.; Sim, M. M. β-Carbolines as specific inhibitors of cyclin-dependent kinases. *Bioorg. Med. Chem. Lett.* **2002**, *12*, 1129−1132.

(13) Li, X.; Huang, P.; Cui, J. J.; Zhang, J.; Tang, C. Novel pyrrolyllactone and pyrrolyllactam indolinones as potent cyclin-dependent kinase 2 inhibitors. *Bioorg. Med. Chem. Lett*. **2003**, *13*, 1939−1942.

(14) Beattie, J. F.; Breault, G. A.; Ellston, R. P. A.; Green, S.; Jewsbury, P. J.; Midgley, C. J.; Naven, R. T.; Minshull, C. A.; Pauptit, R. A.; Tucker, J. A.; Pease, J. E. Cyclin-dependent kinase 4 inhibitors as a treatment for cancer. Part 1: Identification and optimisation of substituted 4,6-bis anilino pyrimidines. *Bioorg. Med. Chem. Lett.* **2003**, *13*, 2955−2960.

(15) Breault, G. A.; Ellston, R. P. A. A.; Green, S.; James, S. R.; Jewsbury, P. J.; Midgley, C. J.; Pauptit, R. A.; Minshull, C. A.; Tucker, J. A.; Pease, J. E. Cyclin-dependent kinase 4 inhibitors as a treatment for cancer. Part 2: Identification and optimisation of substituted 2,4-bis anilino pyrimidines. *Bioorg. Med. Chem. Lett*. **2003**, *13*, 2961−2966.

(16) Tang, J.; Shewchuk, L. M.; Sato, H.; Hasegawa, M.; Washio, Y.; Nishigaki, N. Anilinopyrazole as selective CDK2 inhibitors: Design, synthesis, biological evaluation, and X-ray crystallographic analysis. *Bioorg. Med. Chem. Lett*. **2003**, *13*, 2985−2988.

(17) Anderson, M.; Beattie, J. F.; Breault, G. A.; Breed, J.; Byth, K. F.; Culshaw, J. D.; Ellston, R. P. A.; Green, S.; Minshull, C. A.; Norman, R. A.; Pauptit, R. A.; Stanway, J.; Thomas, A. P.; Jewsbury, P. J. Imidazo[1,2-*a*]pyridines: A potent and selective class of cyclin-dependent kinase inhibitors identified through structure-based hybridization. *Bioorg. Med. Chem. Lett*. **2003**, *13*, 3021−3026.

(18) Witherington, J.; Bordas, V.; Gaiba, A.; Naylor, A.; Rawlings, A. D.; Slingsby, B. P.; Smith, D. G.; Takle, A. K.; Ward, R. W. 6-Heteroaryl-pyrazolo[3,4-*b*]pyridines: potent and selective inhibitors of glycogen synthase kinase-3 (GSK-3). *Bioorg. Med. Chem. Lett*. **2003**, *13*, 3059−3062.

(19) Sayle, K. L.; Bentley, J.; Boyle, F. T.; Calvert, A. H.; Cheng, Y.; Curtin, N. J.; Endicott, J. A.; Golding, B. T.; Hardcastle, R. H.; Jewsbury, P.; Mesguiche, V.; Newell, D. R.; Noble, M. E. M.; Parsons, R. J.; Pratt, D. J.; Wang, L. Z.; Griffin, R. J. Structure-based design of 2-arylamino-4-cyclohexylmethyl-5-nitroso-6-aminopyrimidine inhibitors of cyclin-dependent kinases 1 and 2. *Bioorg. Med. Chem. Lett.* **2003**, *13*, 3079−3082.

(20) Zhang, H. C.; Ye, H.; Conway, B. R.; Derian, C. K.; Addo, M. F.; Kuo, G. H.; Hecker, L. R.; Croll, D. R.; Li, L.; Westover, L.; Xu, J, Z.; Look, R.; Demarest, K. T.; Andrade-Gordon, P.; Damiano, B. P.; Maryanoff, B. E. 3-(7-Azaindolyl)-4-arylmaleimides as potent, selective inhibitors of glycogen synthase kinase-3. *Bioorg. Med. Chem. Lett.* **2004**, *14*, 3245−3250.

(21) Maeda, Y.; Nakano, M.; Sato, H.; Miyazaki, Y.; Schweiker, S. L.; Smith, J. L.; Truesdale, A. T. 4-Acylamino-6-arylfuro[2,3-*d*]pyrimidines: Potent and selective glycogen synthase kinase-3 inhibitors. *Bioorg. Med. Chem. Lett.* **2004**, *14*, 3907−3911.

(22) Wilder, F. V.; Barrett, J. P.; Farina, E. J. Joint-specific prevalence of osteoarthritis of the hand. *Bioorg. Med. Chem. Lett.* **2004**, *14*, 953−957.

(23) Bamford, M. J.; Bailey, N.; Davies, S.; Dean, D. K.; Francis, L.; Panchal, T. A.; Parr, C. A.; Sehmi, S.; Steadman, J. G.; Takle, A. K.; Townsend, J. T.; Wilson, D. M. (1*H*-Imidazo[4,5-*c*]pyridin-2-yl)-1,2,5-oxadiazol-3-ylamine derivatives: Further optimisation as highly potent and selective MSK-1-inhibitors. *Bioorg. Med. Chem. Lett.* **2005**, *15*, 3407−3411.

(24) Williamson, D. S.; Parratt, M. J.; Bower, J. F.; Moore, J. D.; Richardson, C. M.; Dokurno, P.; Cansfield, A. D.; Francis, G. L.; Hebdon, R. J.; Howes, R.; Jackson, P. S.; Lockie, A. M.; Murray, J. B.; Nunns, C. L.; Powles, J.; Robertson, A.; Surgenor, A. E.; Torrance, C. J. Structure-guided design of pyrazolo[1,5-*a*]pyrimidines as inhibitors of human cyclin-dependent kinase 2. *Bioorg. Med. Chem. Lett.* **2005**, *15*, 863−867.

(25) Alessio, R. D.; Bargiotti, A.; Metz, S.; Brasca, M. G.; Cameron, A.; Ermoli, A.; Marsiglio, A.; Polucci, P.; Roletto, F.; Tibolla, M.; Vazquez, M. L.; Vulpetti, A.; Pevarello, P. Structure-guided design of pyrazolo[1,5-*a*]pyrimidines as inhibitors of human cyclin-dependent kinase 2. *Bioorg. Med. Chem. Lett*. **2005**, *15*, 1315−1319.

(26) Lin, R.; Lu, Y.; Wetter, S. K.; Connolly, P. J.; Turchi, I. J.; Murray, W. V.; Emanuel, S. L.; Gruninger, R. H.; Fuentes-Pesquera, A. R.; Adams, M.; Pandey, N.; Moreno-Mazza, S.; Middleton, S. A.; Jolliffe, L. K. 3-Acyl-2,6-diaminopyridines as cyclin-dependent kinase inhibitors: Synthesis and biological evaluation. *Bioorg. Med. Chem. Lett.* **2005**, *15*, 2221−2224.

(27) Richardson, C. M.; Williamson, D. S.; Parratt, M. J.; Borgognoni, J.; Cansfield, A. D.; Dokurno, P.; Francis, G. L.; Howes, R.; Moore, J. D.; Murray, J. B.; Robertson, A.; Surgenor, A. E.; Torrance, C. J. Triazolo[1,5-*a*]pyrimidines as novel CDK2 inhibitors: Protein structure-guided design and SAR. *Bioorg. Med. Chem. Lett.* **2006**, *16*, 1353−1357.

(28) Zaharevitz, D. W.; Gussio, R.; Leost, M.; Senderowicz, A. M.; Lahusen, T.; Kunick, C.; Meijer, L.; Sausville, E. A. Discovery and initial characterization of the paullones, a novel class of small-molecule inhibitors of cyclin-dependent kinases. *Cancer Res.* **1999**, *59*, 2566−2569.

(29) Ruetz, S.; Fabbro, D.; Zimmermann, J.; Meyer, T.; Gray, N. Chemical and biological profile of dual CDK1 and CDK2 Inhibitors. *Curr. Med. Chem. Anti-Cancer Agents.* **2003**, *3*, 1−14.

(30) Fischer, P. M.; Lane, D. P. Inhibitors of cyclin-dependent kinases as anti-cancer therapeutics. *Curr. Med. Chem*. **2000**, *7*, 1213−1245.

(31) Batra, S.; Srinivasan, T.; Rastogi, S. K.; Kundu, B. Identification of enzyme inhibitors using combinatorial libraries. *Curr. Med. Chem*. **2002**, *9*, 307−319.

(32) Sielecki, T. M.; Boylan, J. F.; Benfield, P. A.; Trainor, G. L. Cyclin-dependent kinase inhibitors: Useful targets in cell cycle regulation. *J. Med. Chem.* **2000**, *43*, 1−18.

(33) Shewchuk, L.; Hassell, A.; Wisely, B.; Rocque, W.; Holmes, W.; Veal, J.; Kuyper, L. F. Binding mode of the 4-anilinoquinazoline class of protein kinase inhibitor: X-ray crystallographic studies of 4-anilinoquinazolines bound to cyclin-dependent kinase 2 and p38 kinase. *J. Med. Chem.* **2000**, *43*, 133−138.

(34) Otyepka, M.; Kryštof, V.; Havlíček, L.; Siglerová, V.; Strnad, M.; Koča, J. Docking-based development of purine-like inhibitors of cyclin-dependent kinase-2. *J. Med. Chem.* **2000**, *43*, 2506−2513.

(35) Kim, K. S.; Sack, J. S.; Tokarski, J. S.; Qian, L.; Chao, S. T.; Leith, L.; Kelly, Y. F.; Misra, R. N.; Hunt, J. T.; Kimball, S. D.; Humphreys, W. G.; Wautlet, B. S.; Mulheron, J. G.; Webster, K. R. Thio- and oxoflavopiridols, cyclin-dependent kinase 1-selective inhibitors: Synthesis and biological effects. *J. Med. Chem.* **2000**, *43*, 4126−4134.

(36) Barvian, M.; Boschelli, D. H.; Cossrow, J.; Dobrusin, E.; Fattaey, A.; Fritsch, A.; Fry, D.; Harvey, P.; Keller, P.; Garrett, M.; La, F.; Leopold, W.; McNamara, D.; Quin, M.; Trumpp-Kallmeyer, S.; Toogood, P.; Wu, Z.; Zhang, E. Pyrido[2,3-*d*]pyrimidin-7-one inhibitors of cyclin-dependent kinases. *J. Med. Chem*. **2000**, *43*, 4606−4616.

(37) Honma, T.; Yoshizumi, T.; Hashimoto, N.; Hayashi, K.; Kawanishi, N.; Fukasawa, K.; Takaki, T.; Ikeura, C.; Ikuta, M.; Suzuki-Takahashi, I.; Hayama, T.; Nishimura, S.; Morishima, H. A novel approach for the development of selective CDK4 inhibitors: Library design based on locations of CDK4 specific amino acid residues. *J. Med. Chem.* **2001**, *44*, 4628−4640.

(38) Schoepfer, J.; Fretz, H.; Chaudhuri, B.; Muller, L.; Seeber, E.; Meijer, L.; Lozach, O.; Vangrevelinghe, E.; Furet, P. Structure-based design and synthesis of 2-benzylidene-benzofuran-3-ones as flavopiridol mimics. *J. Med. Chem*. **2002**, *45*, 1741−1747.

(39) Olesen, P. H.; Sørensen, A. R.; Ursø, B.; Kurtzhals, P.; Bowler, A. N.; Ehrbar, U.; Hansen, B. F. Synthesis and in vitro characterization of 1-(4-Aminofurazan-3-yl)-5-dialkylaminomethyl-1H-[1,2,3]triazole-4-carboxylic acid derivatives. A new class of selective GSK-3 inhibitors. *J. Med. Chem.* **2003**, *46*, 3333−3341.

(40) Mettey, Y.; Gompel, M.; Thomas, V.; Garnier, M.; Leost, M.; Ceballos-Picot, I.; Noble, M.; Endicott, J.; Vierfond, J.; Meijer, L.; Aloisines, a new family of CDK/GSK-3 inhibitors. SAR study, crystal structure in complex with CDK2, enzyme selectivity, and cellular effects. *J. Med. Chem.* **2003**, *46*, 222−236.

(41) Pevarello, P.; Brasca, M. G. B.; Amici, R.; Orsini, P.; Traquandi, G.; Corti, L.; Piutti, C.; Sansonna, P.; Villa, M.; Pierce, B. S.; Pulici, M.; Giordano, P.; Martina, K.; Fritzen, E. L.; Nugent, R. A.; Casale, E.; Cameron, A.; Ciomei, M.; Roletto, F.; Isacchi, A.; Fogliatto, G.; Pesenti, E.; Pastori, W.; Marsiglio, A.; Leach, K. L.; Clare, P. M.; Fiorentini, F.; Varasi, M.; Vulpetti, A.; Warpehoski, M. A. 3-Amino-pyrazole inhibitors of CDK2/cyclin A as antitumor agents. 1. Lead finding. *J. Med. Chem.* **2004**, *47*, 3367−3380.

(42) VanderWel, S. N.; Harvey, P. J.; McNamara, D. J.; Repine, J. T.; Keller, P. R.; Quin, J., III; Booth, R. J.; Elliott, W. L.; Dobrusin, E. M.; Fry, D. W.; Toogood, P. L. Pyrido[2,3-*d*]pyrimidin-7-ones as specific inhibitors of cyclin-dependent kinase 4. *J. Med. Chem.* **2005**, *48*, 2371−2387.

(43) Pevarello, P.; Brasca, M. G.; Orsini, P.; Traquandi, G.; Longo, A.; Nesi, M.; Orzi, F.; Piutti, C.; Sansonna, P.; Varasi, M.; Cameron, A.; Vulpetti, A.; Roletto, F.; Alzani, R.; Ciomei, M.; Albanese, C.; Pastori, W.; Marsiglio, A.; Pesenti, E.; Fiorentini, F.; Bischoff, J. R.; Mercurio, C. 3-Aminopyrazole inhibitors of CDK2/cyclin A as antitumor agents. 2. Lead optimization. *J. Med. Chem.* **2005**, *48*, 2944−2956.

(44) Putta, S.; Landrum, G. A.; Penzotti, J. E. Conformation mining: An algorithm for finding biologically relevant conformations. *J. Med. Chem.* **2005**, *48*, 3313−3318.

(45) *Catalyst*, version 4.11; Accelrys Inc: San Diego, CA, 2005.

(46) Debnath, A. K. Pharmacophore mapping of a series of 2,4-diamino-5-deazapteridine inhibitors of *Mycobacterium avium* complex dihydrofolate reductase. *J. Med. Chem.* **2002**, *45*, 41−53.

(47) Berman, H. M.; Westbrook, J.; Feng, Z.; Gilliland, G.; Bhat, T. N.; Weissig, H.; Shindyalov, I. N.; Bourne, P. E. The protein data bank. *Nucleic Acids Res.* **2000**, *28*, 235−242.
(48) *Cerius*^{2}, version 4.11; Accelrys Inc: San Diego, CA, 2005.
(49) Jones, G.; Willett, P.; Glen, R. C. Molecular recognition of receptor sites using a genetic algorithm with a description of desolvation. *J. Mol. Biol*. **1995**, *245*, 43−53.
(50) Hirashima, A.; Morimoto, M.; Kuwano, E.; Taniguchi, E.; Eto, M. Three-Dimensional Common-Feature Hypotheses for Octopamine Agonist 2-(Arylimino)imidazolidines. *Bioorg. Med. Chem.* **2002**, *10*, 117−23.
(51) Osman, F. Guner.; Douglas, R. Henry. Metric for analyzing hit lists and pharmacophores. In *Phamacophore Perception, Development, and Use in Drug Design*; Guner., O. F., Ed.; International University Line: La Jolla, CA, 2000; pp 193−210.

CI7000742